Defence Research and Development Canada
Recherche et développement pour la défense Canada

DEFENCE R&D DÉFENSE

MIMO radar search strategies for high-velocity targets

Peter W. Moo

Defence R&D Canada – Ottawa

Canada

Technical Memorandum
DRDC Ottawa TM 2009-288
March 2010

MIMO radar search strategies for high-velocity targets

Peter W. Moo
Defence R&D Canada – Ottawa

Defence R&D Canada – Ottawa
Technical Memorandum
DRDC Ottawa TM 2009-288
March 2010

Principal Author

Original signed by Peter W. Moo

Peter W. Moo

Approved by

Original signed by A. Damini

A. Damini
A/Head/RS

Approved for release by

Original signed by B. Eatock

B. Eatock
Head/Document Review Panel

Abstract

This work considers the detection of high-velocity targets for naval phased array radar. The detection performance of multiple-input multiple-output (MIMO) radar with orthogonal waveforms is compared to that of a radar using a directed beam. An analytical expression for the probability of detection for a radar with a multiple element array is derived. For high velocity targets, the decrease in probability of detection due to the longer integration time required for MIMO radar is quantified. It is shown that for lower-velocity targets, sector search using orthogonal waveforms results in higher detection range. For higher-velocity targets, the use of scanning directed beams yields higher detection range.

Résumé

Les présents travaux portent sur la détection de cibles à haute vitesse par les radars à balayage électronique de la Marine. Les performances de détection du radar MIMO (multiple-input multiple-output = entrées et sorties multiples) à formes d'ondes orthogonales sont comparées à celles d'un radar à faisceau dirigé. Une expression analytique de la probabilité de détection par un radar à antenne réseau à multiples éléments est présentée. Pour les cibles à haute vitesse, la diminution de la probabilité de détection en raison de la plus longue période d'intégration nécessaire au radar MIMO est quantifiée. On montre que, pour les cibles à plus faible vitesse, la recherche par secteur au moyen de formes d'ondes orthogonales accroît la portée de détection. Dans le cas des cibles à plus grande vitesse, l'utilisation de faisceaux d'exploration dirigés augmente la portée de détection.

This page intentionally left blank.

Executive summary

MIMO radar search strategies for high-velocity targets

Peter W. Moo; DRDC Ottawa TM 2009-288; Defence R&D Canada – Ottawa; March 2010.

Naval radars have a requirement to detect airborne targets, which may have radar cross sections as low as 0.1 m^2 and velocities as high as Mach 2. In addition, naval vessels are being called upon to operate in littoral regions, which are characterized by dense target environments. Multiple-input multiple-output (MIMO) radar is a novel radar concept that can be considered for naval applications. A MIMO radar has the flexibility to transmit distinct waveforms on multiple transmitters and carry out processing on multiple receivers. This diversity and flexibility has the potential to enhance the detection, tracking and parameter estimation of targets. If a MIMO radar transmits orthogonal waveforms, the directional beam gain is lost and integration time must be increased to maintain signal-to-noise ratio. However, the longer integration times required for MIMO operation may degrade the detection performance for high velocity targets. This work compares the detection performance of a radar using a directed beam mode to that of a radar using orthogonal waveforms.

For a multiple-element antenna array radar, target detection in a single range bin is considered. An analytical expression for the range bin probability of detection is derived. This expression explicitly accounts for the fact that the radar return from a high-velocity target may be spread over multiple range cells. Under the assumption that the radar knows the location of the target, as would be the case for a tracked target, it is shown that the single target probability of detection of a directed beam radar is greater than that of a radar transmitting orthogonal waveforms. A number of examples are presented, and the difference in probability of detection is quantified.

A comparison of sector search performance is also considered for a multiple-element array. In searching for targets within a sector, directed beam search suffers from beam shape loss, beam steering loss, and sector search time lag. These losses are incorporated into a sector search scenario that considers targets with varying velocity, radar cross section, and angle of arrival. The detection range for directed beam and for orthogonal waveforms is compared for each target in the scenario. For stationary and lower-velocity targets, the use of orthogonal waveforms results in higher detection range. For higher-velocity targets, the use of scanning directed beams yields higher detection range. It is also shown that the use of shorter coherent processing intervals enhances detection performance for orthogonal waveforms.

Sommaire

MIMO radar search strategies for high-velocity targets

Peter W. Moo ; DRDC Ottawa TM 2009-288 ; R & D pour la défense Canada – Ottawa ; mars 2010.

Les radars de la Marine ont à détecter des cibles aériennes, lesquelles peuvent avoir de faibles surfaces équivalentes radar et de grandes vitesses. En outre, les navires de la Marine doivent mener des opérations dans les régions littorales, qui sont caractérisées par des environnements à forte densité de cibles. Le radar MIMO est une nouvelle technique radar qui peut être envisagée pour des applications navales. Un radar MIMO a la souplesse voulue pour émettre des formes d'ondes distinctes sur de multiples émetteurs et de traiter les signaux de multiples récepteurs. Cette diversité et cette souplesse peuvent améliorer la détection, la poursuite et l'estimation des paramtres de cibles. Si un radar MIMO émet des formes d'ondes orthogonales, le gain de faisceau dirigé est perdu et la période d'intégration doit être accrue afin de maintenir le rapport signal/bruit. Toutefois, les plus longues périodes d'intégration nécessaires pour l'exploitation du radar MIMO peuvent dégrader les performances de détection des cibles à haute vitesse. Les présents travaux comparent les performances de détection d'un radar à faisceau dirigé et d'un radar à formes d'ondes orthogonales.

Dans le cas d'un radar à antenne réseau à multiples éléments d'antenne, la détection de cibles dans une unique cellule de distance est étudiée. Une expression analytique de la probabilité de détection dans une cellule de distance est présentée. Cette expression tient compte explicitement du fait que l'écho radar d'une cible à haute vitesse peut s'étaler sur de multiples cellules de distance. En supposant que le radar connaît l'emplacement de la cible, on montre que la probabilité de détection d'une cible unique par un radar à faisceau dirigé est plus grande que dans le cas d'un radar à formes d'ondes orthogonales. Un certain nombre d'exemples sont présentés, et la différence de probabilité de détection est quantifiée.

Une comparaison des performances de recherche par secteur est également étudiée pour un réseau à éléments multiples. Lors de recherches de cibles dans un secteur, le faisceau dirigé accuse une perte de forme, une perte d'orientation et un décalage du temps de recherche. Ces pertes sont incorporées dans un scénario de recherche par secteur tenant compte de cibles à vitesses variées, de la surface équivalente radar et de l'angle d'arrivée. La portée de détection pour le faisceau dirigé et les formes d'ondes orthogonales est comparée pour chaque cible dans le scénario. Dans le cas des cibles fixes et à plus faible vitesse, la recherche par secteur au moyen de formes d'ondes orthogonales accroît la portée de détection. Dans le cas des cibles à plus grande vitesse, l'utilisation de faisceaux d'exploration dirigés augmente la portée de détection. On montre également que l'utilisation d'intervalles de répétition plus courts améliore les performances de détection dans le cas

des formes d'ondes orthogonales.

This page intentionally left blank.

Table of contents

List of figures

List of tables

1 Introduction

Naval radars have a requirement to detect airborne targets, such as cruise missiles and low-flying aircraft. These targets may be difficult to detect due to their small radar cross sections and high velocities. Because naval vessels are increasingly operating in littoral environments, the radar must be able to detect these threats in dense target environments. The challenge of detection in dense target environments leads to the consideration of multiple-input multiple-output (MIMO) radar for naval applications.

A MIMO radar exploits the diversity and flexibility of multiple transmitters and multiple receivers to enhance the detection, tracking and parameter estimation of targets. A key element of MIMO radar is the simultaneous transmission of orthogonal waveforms by the transmitters and the corresponding advanced signal processing that must be carried out by the receivers to exploit the diversity of the transmitted waveforms. In general, a MIMO radar may be a monostatic or a multistatic system. A comprehensive literature review of MIMO radar was given in [1]. In this work, a monostatic MIMO radar is considered. Rabideau and Parker [2] proposed an ubiquitous radar architecture, whereby each array element transmits a low-gain signal to illuminate a broad surveillance area. Bekkerman and Tabrikian [3] considered the use of orthogonal waveforms for the array elements and showed that this resulted in enhanced target detection and localization performance compared to the use of a directed beam. In van Rossum and Huizing [4], four radar array concepts were compared, including pencil beam, floodlight, monostatic MIMO, and multistatic MIMO. Detection performance for the concepts was analyzed using simulation. Li et al. [5] show that a radar which transmits M orthogonal waveforms can uniquely identify M times as many targets as a radar that uses a directed beam. Identification typically requires more signal-to-noise ratio than detection. These results are motivation for the great interest in MIMO radar.

The use of MIMO radar for naval applications requires that the radar detect high-velocity targets. Although an M-element MIMO radar has the flexibility to transmit M orthogonal waveforms simultaneously, an M-element phased array antenna that transmits a directional beam (i.e. coherent transmission) will have a beam gain that is M times higher than the MIMO radar. As a result, the MIMO radar must dwell on the target M times longer to maintain the same signal-to-noise ratio [3]. In dense target environments, MIMO radar may be able to detect more targets simultaneously than a directional beam. However, the longer integration times required for MIMO operation may degrade the detection performance for high velocity targets. This work compares the detection performance of a radar using a directed beam mode to that of a radar using orthogonal waveforms and explicitly considers the effects of longer dwell times on probability of detection.

The outline of this memorandum is as follows. In Section 2, the system model for a radar array with M elements is specified. Section 3 presents the derivation of an analytical expression for the probability of detection and the probability of false alarm. In Section 4,

single target probability of detection for a directed beam radar is compared to that for a radar using orthogonal waveforms. Search strategies are analyzed and discussed in Section 5. Finally, conclusions are presented in Section 6.

2 System Model

This section summarizes the signal model from Bekkerman and Tabrikan [3]. The radar is an M-element antenna array, where each element transmits a narrow-band signal. The samples of the baseband equivalent signals are given by $\{s[n]\}_{n=1}^{N}$ where n is the time index, s is an M-dimensional vector, and the m-th element $\{s_m[n]\}_{n=1}^{N}$ are the samples for element m. The coherence matrix is given by

$$\begin{aligned} R &= \frac{1}{N}\sum_{n=1}^{N} s[n]s^H[n] \\ &= \begin{bmatrix} 1 & \beta_{12} & \cdots & \beta_{1M} \\ \beta_{21} & 1 & \cdots & \beta_{2M} \\ \vdots & \vdots & \ddots & \vdots \\ \beta_{M1} & \beta_{M2} & \cdots & 1 \end{bmatrix}, \end{aligned}$$

where β_{ij} is the complex correlation coefficient between signals i and j, and ^{H} is the Hermitian operation. For a directed beam, the rank of R is equal to one, because the different elements transmit the same signal with phase shifts to steer the beam. For orthogonal transmission, R is the identity matrix by definition, because the transmitted signals are uncorrelated. It is assumed that an ideal directed beam and ideal orthogonal transmission can be achieved by the radar. For a single target located at direction θ, the received signal by element m is given by

$$y_m[n] = \alpha\sum_{i=1}^{M} A_{im}(\theta)s_i[n] + w_m[n], \tag{1}$$

where $m = 1,...,M$, $n = 1,...,N$, α is the complex amplitude of the received signal, $w_m[n]$ is the additive noise at the m-th element, and $A_{im}(\theta)$ is the total phase delay of the signal transmitted by element i and received by element m. Define $A(\theta)$ as the M-by-M array response matrix where the im-th element is $A_{im}(\theta)$, $w[n]$ as the M-by-1 additive noise vector where the m-th element is $w_m[n]$, and $y[n]$ as the M-by-1 received signal vector where the m-th element is $y_m[n]$. The noise vector $w[n]$ is zero-mean complex Gaussian with covariance matrix $R_w = 2\sigma^2 I_M$. The signal received by the antenna array can then be expressed as

$$y[n] = z[n] + w[n], \tag{2}$$

where $z[n] = \alpha A(\theta)s[n]$.

3 Analytical Expression for Probability of Detection

When orthogonal waveforms are used, each element transmits omnidirectionally, so that the beam gain is less than the beam gain for the directional beam. If all other radar parameters are equal, a radar transmitting orthogonal waveforms must dwell longer on the target than a radar using a directed beam to maintain the same signal-to-noise ratio.

The radar samples the received signal so that the received signal is divided into a series of range cells. For a target with non-zero velocity, the target return may be spread over multiple range cells. This will depend on the relationship between range cell length and the distance the target travels during the coherent processing interval (CPI). In the derivation that follows, probability of detection will be computed for a single range cell. If the target return is spread over multiple range cells, then probability of detection will be computed for the range cell with the strongest target return. In this way, the derivation explicitly accounts for the longer dwell time used for orthogonal waveforms. The following terms will be used in the derivation.

- ρ is the length of the range cell in meters,
- v is the radial velocity of the target,
- Λ is the length of the CPI for the directed beam, in seconds,
- α is the distance traveled by the target during the CPI.

When the radar uses a directed beam, $\alpha_{\text{dir}} = v\Lambda$. If orthogonal waveforms are used, then $\alpha_{\text{orth}} = vM\Lambda$.

Recall the signal model specified in (2). To simplify the derivation, the M-dimensional complex vector $y[n]$ is specified as a $2M$-dimensional real vector $\tilde{y}[n]$, where the real and imaginary components of each element of $y[n]$ are the elements of $\tilde{y}[n]$. Similarly, the vectors $z[n]$ and $w[n]$ are specified as $\tilde{z}[n]$ and $\tilde{w}[n]$. The following arithmetic means are also computed: $\underline{y} = \frac{1}{N}\sum_{n=1}^{N}\tilde{y}[n]$, $\underline{z} = \frac{1}{N}\sum_{n=1}^{N}\tilde{z}[n]$, and $\underline{w} = \frac{1}{N}\sum_{n=1}^{N}\tilde{w}[n]$.

For single target detection, the radar must decide between two hypotheses,

$$\begin{aligned} H_0 &: \underline{y} = \underline{w}, \\ H_1 &: \underline{y} = \underline{z} + \underline{w}, \end{aligned}$$

where is $\underline{z}$ is a 2M-dimensional real vector representing the target return and $\underline{w}$ is a zero-mean 2M-dimensional real Gaussian vector with covariance matrix $R_{\underline{w}} = \sigma^2 I_{2M}$. A threshold detector can be expressed as

$$\|\underline{y}\| \gtrless_{H_0}^{H_1} \gamma, \tag{3}$$

where the threshold γ is chosen to satisfy a specified probability of false alarm P_{fa}, that is,

$$\Pr(\|\underline{w}\| > \gamma) = P_{\text{fa}}. \tag{4}$$

An expression for the left-hand side of (4) will be developed in Section 3.2.

Consider a single range cell, where by definition ρ is the length in meters. It is assumed that the target may originate with equal probability at any location in the range cell. That is, the random variable r is the starting location of the target in the range cell and has a uniform distribution, so that the probability density function is $p(r) = 1/\rho, 0 \leq r \leq \rho$. The probability of detection for a target in the range cell will depend on the total signal power contained in the range cell. Let c be the largest fraction of total signal power contained in any range cell, where $0 \leq c \leq 1$. Expressions for c as a function of r will be presented in Section 3.3.

The probability of detection in a range cell as a function of c is given by

$$\begin{aligned} \eta(c) &= \Pr(\|c\,\underline{z} + \underline{w}\| > \gamma) && (5) \\ &= \int_{\|\underline{w}\|=\gamma}^{\|\underline{w}\|=\infty} \frac{1}{(2\pi\sigma^2)^M} e^{-\frac{1}{2\sigma^2}\|\underline{w}-c\underline{z}\|^2} d\underline{w} && (6) \end{aligned}$$

3.1 Derivation of Probability of Detection for fixed c

In order to evaluate the probability of detection for a M-element array, $\eta(c)$ must be evaluated. However the right hand side of (6) does not have a closed form solution, since the integral cannot be evaluated exactly. In this subsection, an approximation to (6) will be derived. Starting with (6), we have

$$\begin{aligned} \eta(c) &= 1 - \frac{1}{(2\pi\sigma^2)^M} \int_{\|\underline{w}'\|=0}^{\|\underline{w}'\|=\gamma} e^{-\frac{1}{2\sigma^2}\|\underline{w}'-c\underline{z}\|^2} d\underline{w}' \\ &= 1 - \frac{1}{(2\pi\sigma^2)^M} I && (7) \end{aligned}$$

where

$$I = \int_A e^{-\frac{1}{2\sigma^2}\|\underline{w}\|^2} d\underline{w},$$

$A = \{\underline{w} : 0 \leq \|\underline{w} + c\underline{z}\| \leq \gamma\}$, and (7) follows from the change of variables $\underline{w} = \underline{w}' - c\underline{z}$.

Next, the coordinate system is changed to hyperspherical coordinates, which is a generalization to dimensions greater than three of polar coordinates in two dimensions and spherical coordinates in three dimensions. For $\underline{w} = [w_1 w_2 \cdots w_{2M}]^T$, the hyperspherical

coordinates $r, \phi_1, \phi_2, ..., \phi_{2M-1}$ satisfy

$$\begin{aligned} w_1 &= r\cos(\phi_1) \\ w_2 &= r\sin(\phi_1)\cos(\phi_2) \\ w_3 &= r\sin(\phi_1)\sin(\phi_2)\cos(\phi_3) \\ &\vdots \\ w_{2M-1} &= r\sin(\phi_1)\cdots\sin(\phi_{2M-2})\cos(\phi_{2M-1}) \\ w_{2M} &= r\sin(\phi_1)\cdots\sin(\phi_{2M-2})\sin(\phi_{2M-1}) \end{aligned}$$

The hyperspherical coordinates consist of a radial coordinate r and $2M-1$ angular coordinates $\phi_1, \phi_2, ..., \phi_{2M-1}$, where angles $\phi_1, ..., \phi_{2M-2}$ have a range of 0 to π, and angle ϕ_{2M-1} has a range of 0 to 2π. The volume element in these coordinates is given by

$$\left| \frac{\partial(w_1, w_2, ..., w_{2M})}{\partial(r, \phi_1, ..., \phi_{2M-1})} \right| = r^{2M-1} \prod_{j=1}^{2M-2} \left[\sin(\phi_j)\right]^{2M-1-j}. \tag{8}$$

The vector $\underline{z} = [z_1 z_2 \cdots z_{2M}]^T$ represents the target return and can be expressed in hyperspherical coordinates $\hat{r}, \hat{\phi}_1, \hat{\phi}_2, ..., \hat{\phi}_{2M-1}$ where

$$\begin{aligned} \hat{r} &= \sqrt{z_1^2 + z_2^2 + \cdots + z_{2M}^2} \\ \hat{\phi}_{2M-1} &= \arctan\left(\frac{z_{2M}}{z_{2M-1}}\right) \\ \hat{\phi}_{2M-2} &= \arctan\left(\frac{\sqrt{z_{2M}^2 + z_{2M-1}^2}}{z_{2M-2}}\right) \\ &\vdots \\ \hat{\phi}_1 &= \arctan\left(\frac{\sqrt{z_{2M}^2 + z_{2M-1}^2 + \cdots + z_2^2}}{z_1}\right) \end{aligned} \tag{9}$$

The scaled vector $c\underline{z}$ has hyperspherical coordinates $c\hat{r}, \hat{\phi}_1, \hat{\phi}_2, ..., \hat{\phi}_{2M-1}$ since the angle coordinates are invariant to scaling. Define

$$B = \{r, \phi_1, ..., \phi_{2M-1} : c\hat{r} - \gamma \le r \le c\hat{r} + \gamma, \},$$

for $c\|\underline{z}\| > \gamma$. The following shows that $A \subset B$. Consider any $\underline{w} \in A$. By definition, $0 \le \|\underline{w} + c\underline{z}\| \le \gamma$. Express $\underline{w} = \underline{w} + c\underline{z} - c\underline{z}$. Using the triangle inequality yields

$$\begin{aligned} \|\underline{w}\| &\le \|\underline{w} + c\underline{z}\| + \|c\underline{z}\| \\ &\le \gamma + \|c\underline{z}\| \end{aligned}$$

Similarly, express $c\underline{z} = -\underline{w} + \underline{w} + c\underline{z}$. Again the use of the triangle inequality shows that

$$\begin{aligned} \|c\underline{z}\| &\leq \|\underline{w}\| + \|\underline{w} + c\underline{z}\| \\ &\leq \|\underline{w}\| + \gamma, \end{aligned}$$

which shows that $\|\underline{w}\| \geq \|c\underline{z}\| - \gamma$. Therefore $\underline{w} \in B$, which shows that $A \subset B$.

Returning to (7),

$$\begin{aligned} I &= \int_A e^{-\frac{1}{2\sigma^2}\|\underline{w}\|^2} d\underline{w} \\ &\leq \int_B e^{-\frac{1}{2\sigma^2}\|\underline{w}\|^2} d\underline{w} \qquad (10) \\ &= \int_{\phi_{2M-1}=0}^{\phi_{2M-1}=2\pi} \int_{\phi_{2M-2}=0}^{\phi_{2M-2}=\pi} \cdots \int_{\phi_2=0}^{\phi_2=\pi} \int_{\phi_1=0}^{\phi_1=\pi} \int_{r=c\hat{r}-\gamma}^{r=c\hat{r}+\gamma} e^{-r^2/2\sigma^2} r^{2M-1} \\ &\quad \cdot \sin^{2M-2}(\phi_1) \sin^{2M-3}(\phi_2) \cdots \sin(\phi_{2M-2}) \\ &\quad \cdot dr\, d\phi_1\, d\phi_2 \cdots d\phi_{2M-2}\, d\phi_{2M-1} \qquad (11) \\ &= \int_{r=c\hat{r}-\gamma}^{r=c\hat{r}+\gamma} e^{-r^2/2\sigma^2} dr \int_{\phi_1=0}^{\phi_1=\pi} \sin^{2M-2}(\phi_1) d\phi_1 \\ &\quad \int_{\phi_2=0}^{\phi_2=\pi} \sin^{2M-3}(\phi_2) d\phi_2 \cdots \int_{\phi_{2M-2}=0}^{\phi_{2M-2}=\pi} \sin(\phi_{2M-2}) d\phi_{2M-2} \\ &\quad \int_{\phi_{2M-1}=0}^{\phi_{2M-1}=2\pi} d\phi_{2M-1} \qquad (12) \\ &= J_{2M-1}(c\hat{r}-\gamma, c\hat{r}+\gamma) \left[\prod_{j=1}^{2M-2} I_j(0,\pi) \right] I_{2M-1}(0,2\pi), \qquad (13) \end{aligned}$$

where (10) follows from $A \subset B$, (11) follows from the change to hyperspherical coordinates, and (12) follows because the integrand is a product of functions of the integration variables. The terms in (13) are defined by

$$\begin{aligned} J_{2M-1}(a,b) &= \int_a^b r^{2M-1} e^{-r^2/2\sigma^2} dr \\ I_j(a,b) &= \int_a^b \left[\sin(\phi_j)\right]^{2M-1-j} d\phi_j, j = 1, ..., 2M-1. \end{aligned}$$

3.1.1 Evaluation of I_j integrals

To evaluate the $I_j(0,\pi)$ terms for $j = 1, ..., 2M-2$ in (13), a recursive equation for the integral of $\sin^n x$ is developed. Integrate by parts using

$$\begin{aligned} f &= \sin^{n-1} x \qquad g = -\cos x, \\ f' &= (n-1)\sin^{n-2} x \cos x\, dx \qquad g' = \sin x\, dx. \end{aligned}$$

This yields

$$\begin{aligned}\int_a^b \sin^n x\,dx &= -\sin^{n-1} x\cos x\Big|_a^b + (n-1)\int_a^b \sin^{n-2} x\cos^2 x\,dx \\ &= -\sin^{n-1} x\cos x\Big|_a^b + (n-1)\int_a^b \sin^{n-2} x(1-\sin^2 x)\,dx \qquad (14)\end{aligned}$$

Adding $(n-1)\int_a^b \sin^n x\,dx$ to both sides of (14) yields

$$\int_a^b \sin^n x\,dx + (n-1)\int_a^b \sin^n x\,dx = -\sin^{n-1} x\cos x\Big|_a^b + (n-1)\int_a^b \sin^{n-2} x\,dx.$$

Dividing by n gives the recursive equation

$$\int_a^b \sin^n x\,dx += -\frac{1}{n}\sin^{n-1} x\cos x\Big|_a^b + \frac{(n-1)}{n}\int_a^b \sin^{n-2} x\,dx. \qquad (15)$$

Evaluating (15) recursively yields

$$\begin{aligned}\int_a^b \sin^n x\,dx &= -\frac{1}{n}\sin^{n-1} x\cos x\Big|_a^b - \frac{n-1}{n}\frac{1}{n-2}\sin^{n-3} x\cos x\Big|_a^b \\ &\quad + \frac{n-1}{n}\frac{n-3}{n-2}\int_a^b \sin^{n-4} x\,dx \\ &= -\frac{1}{n}\sin^{n-1} x\cos x\Big|_a^b - \frac{n-1}{n}\frac{1}{n-2}\sin^{n-3} x\cos x\Big|_a^b \\ &\quad - \frac{n-1}{n}\frac{n-3}{n-2}\frac{1}{n-4}\sin^{n-5} x\cos x\Big|_a^b + \frac{n-1}{n}\frac{n-3}{n-2}\frac{n-5}{n-4}\int_a^b \sin^{n-6} x\,dx.\end{aligned}$$

The expression continues recursively until the last term is reached. If n is even, the last term is

$$\frac{(n-1)!!}{n!!}\int_a^b dx = \frac{(n-1)!!}{n!!}(b-a).$$

where the double factorial is defined by $n!! = n\cdot(n-2)!!$ for integer $n \geq -1$ and where $2!! = 2$, $1!! = 1$ and $0!! = (-1)!! = 1$. If n is odd, the last term is

$$\frac{(n-1)!!}{n!!}\int_a^b \sin x\,dx = \frac{(n-1)!!}{n!!}(\cos a - \cos b).$$

In total we have

$$\begin{aligned}\int_a^b \sin^n x\,dx &= -\sum_{j=1}^{\lfloor \frac{n}{2} \rfloor}\frac{(n-2j)!!}{n!!}\frac{(n-1)!!}{(n+1-2j)!!}\sin^{n+1-2j} x\cos x\Big|_a^b \\ &\quad + \frac{(n-1)!!}{n!!}\left[(b-a)1_{n\,\text{even}} + (\cos a - \cos b)1_{n\,\text{odd}}\right], \qquad (16)\end{aligned}$$

where $1_{n\,\text{even}}$ equals one if n is even and zero if n is odd. Likewise, $1_{n\,\text{odd}}$ equals one if n is odd and zero if n is even. Using (16) it is evident that for $1 \leq j \leq 2M-2$,

$$\begin{aligned} I_j(0,\pi) &= \int_0^{\pi} \left[\sin(\phi_j)\right]^{2M-1-j} d\phi_j \\ &= \frac{(2M-2-j)!!}{(2M-1-j)!!} \left[\pi \cdot 1_{n\,\text{even}} + 2 \cdot 1_{n\,\text{odd}}\right]. \end{aligned}$$

Therefore,

$$\begin{aligned} \left[\prod_{j=1}^{2M-2} I_j(0,\pi)\right] &= (2\pi)^{M-1} \prod_{j=1}^{2M-2} \frac{(j-1)!!}{j!!} \\ &= (2\pi)^{M-1} \frac{1}{(2M-2)!!} \\ &= \frac{(2\pi)^{M-1}}{2^{M-1}(M-1)!} \\ &= \frac{\pi^{M-1}}{(M-1)!}. \end{aligned} \tag{17}$$

It is evident that

$$I_{2M-1}(0,2\pi) = \int_0^{2\pi} d\phi_j = 2\pi. \tag{18}$$

3.1.2 Evaluation of J_{2M-1} integral

Define the integral

$$J_n(a,b) = \int_a^b r^n e^{-r^2/2\sigma^2} dr,$$

for integer n. The integral J_{2M-1} is given by

$$J_{2M-1}(a,b) = \int_a^b r^{2M-1} e^{-r^2/2\sigma^2} dr.$$

Integrate by parts using

$$f = \sigma^2 e^{-r^2/2\sigma^2} \qquad g = -r^{2M-2}, \tag{19}$$

$$f' = -r e^{-r^2/2\sigma^2} dr \qquad g' = -(2M-2) r^{2M-3} dr. \tag{20}$$

This yields

$$\begin{aligned} J_{2M-1}(a,b) &= -\sigma^2 r^{2M-2} e^{-r^2/2\sigma^2}\Big|_a^b + \sigma^2 (2M-2) \int_a^b r^{2M-3} e^{-r^2/2\sigma^2} dr \\ &= -\sigma^2 r^{2M-2} e^{-r^2/2\sigma^2}\Big|_a^b + \sigma^2 (2M-2) J_{2M-3}, \end{aligned} \tag{21}$$

so that (21) is a recursive integral equation. The next two steps in the recursion are given by

$$\begin{aligned} J_{2M-1}(a,b) &= -\sigma^2 r^{2M-2} e^{-r^2/2\sigma^2}\Big|_a^b - \left[\sigma^2\right]^2 (2M-2) r^{2M-4} e^{-r^2/2\sigma^2}\Big|_a^b \\ &\quad + \left[\sigma^2\right]^2 (2M-2)(2M-4), J_{2M-5}, \\ &= -\sigma^2 r^{2M-2} e^{-r^2/2\sigma^2}\Big|_a^b - \left[\sigma^2\right]^2 (2M-2) r^{2M-4} e^{-r^2/2\sigma^2}\Big|_a^b \\ &\quad - \left[\sigma^2\right]^3 (2M-2)(2M-4) r^{2M-6} e^{-r^2/2\sigma^2}\Big|_a^b \\ &\quad + \left[\sigma^2\right]^3 (2M-2)(2M-4)(2M-6) J_{2M-7}, \end{aligned}$$

and the recursions continue until the term J_1 which is evaluated directly as

$$J_1(a,b) = \int_a^b r e^{-r^2/2\sigma^2} dr = -\sigma^2 e^{-r^2/2\sigma^2}\Big|_a^b. \tag{22}$$

Therefore J_{2M-1} is given by

$$J_{2M-1}(a,b) = -\sum_{j=1}^{M} \left(\sigma^{2j} \prod_{k=1}^{j-1} 2(M-k) \right) r^{2(M-j)} e^{-r^2/2\sigma^2}\Big|_a^b. \tag{23}$$

Combining (7), (13), (17), (18), and (23) yields

$$\begin{aligned} \eta(c) &\cong 1 - \frac{1}{2^{M-1}\sigma^{2M}(M-1)!} \sum_{j=1}^{M} \left\{ \left(\sigma^{2j} \prod_{k=1}^{j-1} 2(M-k) \right) \right. \\ &\quad \left. \cdot \left[(c\|\underline{z}\| - \gamma)^{2(M-j)} e^{-(c\|\underline{z}\|-\gamma)^2/2} - (c\|\underline{z}\| + \gamma)^{2(M-j)} e^{-(c\|\underline{z}\|+\gamma)^2/2} \right] \right\}. \end{aligned} \tag{24}$$

Although the expression on the right-hand side of (24) is a lower bound, it will be used as an approximation to $\eta(c)$. This expression relies on the assumption that $c\|\underline{z}\| > \gamma$.

3.2 Derivation of Probability of False Alarm

For the threshold detector in (3), the probability of false alarm is given by

$$\begin{aligned}
\Pr(\|\underline{w}\| > \gamma) &= \frac{1}{(2\pi\sigma^2)^M} \int_{\|\underline{w}\|=\gamma}^{\|\underline{w}\|=\infty} e^{-\frac{1}{2\sigma^2}\|\underline{w}\|^2} d\underline{w} \\
&= \frac{1}{(2\pi\sigma^2)^M} \int_{\phi_{2M-1}=0}^{\phi_{2M-1}=2\pi} \int_{\phi_{2M-2}=0}^{\phi_{2M-2}=\pi} \cdots \int_{\phi_2=0}^{\phi_2=\pi} \int_{\phi_1=0}^{\phi_1=\pi} \int_{r=\gamma}^{r=\infty} e^{-r^2/2\sigma^2} r^{2M-1} \\
&\quad \cdot \sin^{2M-2}(\phi_1) \sin^{2M-3}(\phi_2) \cdots \sin(\phi_{2M-2}) \\
&\quad \cdot dr\, d\phi_1\, d\phi_2 \cdots d\phi_{2M-2}\, d\phi_{2M-1} \qquad (25) \\
&= \frac{1}{(2\pi\sigma^2)^M} \int_{r=\gamma}^{r=\infty} e^{-r^2/2\sigma^2} dr \int_{\phi_1=0}^{\phi_1=\pi} \sin^{2M-2}(\phi_1) d\phi_1 \\
&\quad \int_{\phi_2=0}^{\phi_2=\pi} \sin^{2M-3}(\phi_2) d\phi_2 \cdots \int_{\phi_{2M-2}=0}^{\phi_{2M-2}=\pi} \sin(\phi_{2M-2}) d\phi_{2M-2} \\
&\quad \int_{\phi_{2M-1}=0}^{\phi_{2M-1}=2\pi} d\phi_{2M-1} \qquad (26) \\
&= \frac{1}{(2\pi\sigma^2)^M} J_{2M-1}(\gamma,\infty) \left[\prod_{j=1}^{2M-2} I_j(0,\pi) \right] I_{2M-1}(0,2\pi), \qquad (27)
\end{aligned}$$

where (25) follows from a change to hyperspherical coordinates and (26) follows because the integrand is a product of functions of the integration variables. From (23) it is seen that

$$J_{2M-1}(\gamma,\infty) = \sum_{j=1}^{M} \left(\sigma^{2j} \prod_{k=1}^{j-1} 2(M-k) \right) \gamma^{2(M-j)} e^{-\gamma^2/2\sigma^2}. \qquad (28)$$

Combining (27), (28), (17), and (18) yields

$$\begin{aligned}
\Pr(\|\underline{w}\| > \gamma) &= \frac{1}{(2\pi\sigma^2)^M} \frac{2\pi^M}{(M-1)!} \sum_{j=1}^{M} \left(\sigma^{2j} \prod_{k=1}^{j-1} 2(M-k) \right) \gamma^{2(M-j)} e^{-\gamma^2/2\sigma^2} \\
&= \frac{1}{2^{M-1}\sigma^{2M}(M-1)!} e^{-\gamma^2/2\sigma^2} \sum_{j=1}^{M} \left(\sigma^{2j} \prod_{k=1}^{j-1} 2(M-k) \right) \gamma^{2(M-j)}. \qquad (29)
\end{aligned}$$

3.3 Range cell probability of detection

Range cell probability of detection is given by

$$P_d = \int_0^{\rho} p(r)\eta(c(r))dr = \frac{1}{\rho} \int_0^{\rho} \eta(c(r))dr \qquad (30)$$

First consider the case where $\alpha \leq \rho$. The fraction c as a function of r is given by

$$c(r) = \begin{cases} 1, & \text{if } 0 \leq r \leq \rho - \alpha \\ \dfrac{\rho - r}{\alpha}, & \text{if } \rho - \alpha < r \leq \rho - \frac{\alpha}{2} \\ 1 - \dfrac{\rho - r}{\alpha}, & \text{if } \rho - \frac{\alpha}{2} < r \leq \rho \end{cases} .$$

Evaluating (30) yields

$$\begin{aligned} P_{\mathrm{d}} &= \frac{1}{\rho}\left[(\rho-\alpha)\,\eta(1) + \int_{\rho-\alpha}^{\rho-\frac{\alpha}{2}} \eta\left(\frac{\rho-r}{\alpha}\right) dr + \int_{\rho-\frac{\alpha}{2}}^{\rho} \eta\left(1-\frac{\rho-r}{\alpha}\right) dr\right] && (31) \\ &= \frac{\rho-\alpha}{\rho}\eta(1) + \frac{2}{\rho}\int_{\rho-\alpha}^{\rho-\frac{\alpha}{2}} \eta\left(\frac{\rho-r}{\alpha}\right) dr && (32) \\ &= \frac{\rho-\alpha}{\rho}\eta(1) + \frac{2\alpha}{\rho}\int_{0.5}^{1} \eta(c)dc, && (33) \end{aligned}$$

where (32) follows from the equality of the two integrals in (31), and (33) follows from the change of variables $c = (\rho - r)/\alpha$.

Next consider the case where $\rho < \alpha \leq 2\rho$. The fraction c as a function of r is given by

$$c(r) = \begin{cases} \dfrac{\rho - r}{\alpha}, & \text{if } 0 \leq r \leq \rho - \frac{\alpha}{2} \\ 1 - \dfrac{\rho - r}{\alpha}, & \text{if } \rho - \frac{\alpha}{2} < r \leq 2\rho - \alpha \\ \dfrac{\rho}{\alpha}, & \text{if } 2\rho - \alpha < r \leq \rho \end{cases} .$$

Evaluating (30) yields

$$\begin{aligned} P_{\mathrm{d}} &= \frac{1}{\rho}\left[\int_{0}^{\rho-\frac{\alpha}{2}} \eta\left(\frac{\rho-r}{\alpha}\right) dr + \int_{\rho-\frac{\alpha}{2}}^{2\rho-\alpha} \eta\left(1-\frac{\rho-r}{\alpha}\right) dr + (\alpha-\rho)\,\eta\left(\frac{\rho}{\alpha}\right)\right] && (34) \\ &= \frac{2}{\rho}\int_{0}^{\rho-\frac{\alpha}{2}} \eta\left(\frac{\rho-r}{\alpha}\right) dr + \frac{\alpha-\rho}{\rho}\eta\left(\frac{\rho}{\alpha}\right) && (35) \\ &= \frac{2\alpha}{\rho}\int_{0.5}^{\frac{\rho}{\alpha}} \eta(c)dc + \frac{\alpha-\rho}{\rho}\eta\left(\frac{\rho}{\alpha}\right), && (36) \end{aligned}$$

where (35) follows from the equality of the two integrals in (34) and (36) follows from the change of variables $c = (\rho - r)/\alpha$.

In the final case, $\alpha > 2\rho$, and $c(r) = \rho/\alpha$ for all r so that

$$P_{\mathrm{d}} = \eta\left(\frac{\rho}{\alpha}\right). \qquad (37)$$

Combining (33), (36) and (37) yields a final expression for probability of detection,

$$P_{\mathrm{d}} = \begin{cases} \dfrac{\rho-\alpha}{\rho}\eta(1) + \dfrac{2\alpha}{\rho}\displaystyle\int_{0.5}^{1}\eta(c)dc, & \text{if } \alpha \le \rho \\ \dfrac{2\alpha}{\rho}\displaystyle\int_{0.5}^{\frac{\rho}{\alpha}}\eta(c)dc + \dfrac{\alpha-\rho}{\rho}\eta\left(\dfrac{\rho}{\alpha}\right), & \text{if } \rho < \alpha \le 2\rho \\ \eta\left(\dfrac{\rho}{\alpha}\right), & \text{if } \alpha > 2\rho \end{cases} . \tag{38}$$

The integrals in (38) can be evaluated numerically.

4 Probability of Detection for a Single Target

In this section, detection performance for a single target will be compared for the two radar modes, directed beam and orthogonal waveform. It is assumed that the location of the target is known, so that the radar is not required to search a specified area. This would be the case for a tracked target. For directed beam mode, it is assumed that the target is located in the center of the mainbeam. The probability of false alarm (P_{fa}) is set to 10^{-5}.

The probability of detection is computed as follows. The antenna is an M-element array. The radial velocity of the target is v, and the length of the CPI for the directed beam in seconds is Λ. The probability of detection for directed beam mode is obtained by evaluating (38) with $\alpha = v\Lambda$. The length of the CPI for orthogonal waveforms is $M\Lambda$. Therefore the probability of detection for orthogonal waveform mode is obtained by evaluating (38) with $\alpha = vM\Lambda$.

4.1 Effect of Target Motion on Probability of Detection for Directed Beam Mode

For directed beam mode, Figure 1 shows the probability of detection for a 10-element array when the PRF is 10 kHz, each CPI has 32 pulses, and the range cell length is 30 m. The plots show probability of detection for target radial velocities of 0 m/s, 500 m/s, 1000 m/s, and 1500 m/s. If a SNR of 10 dB is achieved, then probability of detection for a target with zero radial velocity is essentially one, whereas probability of detection is 0.88 for a target with a radial velocity of 1,500 m/s.

4.2 Comparison of Directed Beam to Orthogonal Waveforms

It is evident from examination of (38) that probability of detection performance varies with the relationship between α, the distance travelled by the target during the CPI, and ρ, the length of the range cell. Each of the three scenarios considered in this section have been chosen to illustrate how probability of detection varies for different ratios of α_{dir}, the distance travelled by the target during the directed beam CPI, to ρ. For orthogonal waveforms, $\alpha_{\text{orth}} = M\,\alpha_{\text{dir}}$.

4.2.1 Scenario 1

In Scenario 1, $\alpha_{\text{dir}}/\rho = 0.027$. The PRF is 10 kHz and the target radial velocity v is 250 m/s. For a directed beam, each CPI has 32 pulses, so that the CPI length is 3.2 ms. For antennas with 8, 16 and 24 elements, probability of detection for a directed beam will be

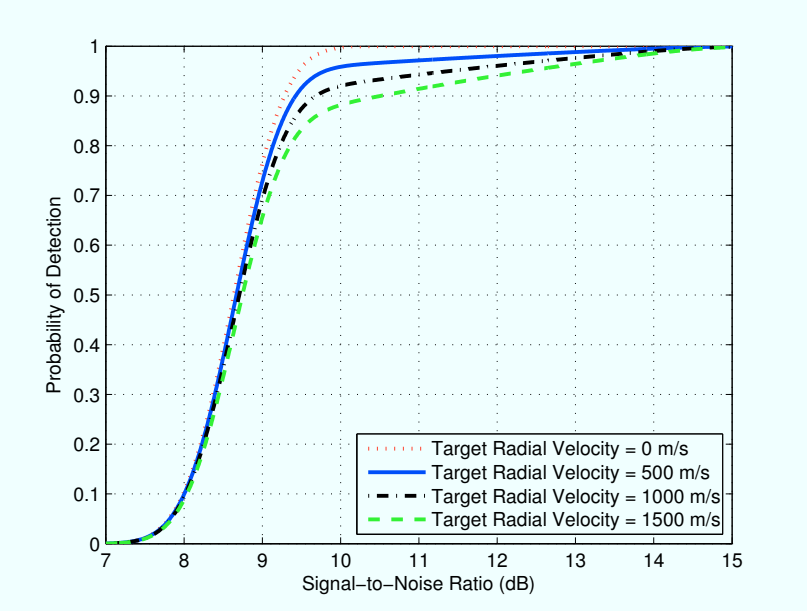

Figure 1: *Probability of detection for an 10-element array in directed beam mode for* $P_{\text{fa}} = 10^{-5}$, $\rho = 30m$ *and a CPI length of 3.2 ms.*

compared to probability of detection for orthogonal waveforms. Table 1 shows the values of α and ρ.

Table 1: *Scenario 1: Distance travelled by the target during the CPI* (α) *and range cell length* (ρ)*, in meters.*

Directed Beam	$\alpha_{\text{dir}} = 0.8$
Orthogonal Waveform (M=8)	$\alpha_{\text{orth}} = 6.4$
Orthogonal Waveform (M=16)	$\alpha_{\text{orth}} = 12.8$
Orthogonal Waveform (M=24)	$\alpha_{\text{orth}} = 19.2$
Range cell length	$\rho = 30$

From (38) it is seen that probability of detection depends on the relationship between α and ρ. In particular, the expression has three distinct cases, $\alpha \leq \rho$, $\rho < \alpha \leq 2\rho$, and $\alpha > 2\rho$. For Scenario 1, $\alpha \leq \rho$ for the directed beam mode and for the orthogonal waveform mode with all three choices of M.

For an 8-element array, Figure 2 compares the probability of detection for the directed beam mode to the probability of detection for the orthogonal waveform mode as a function of signal-to-noise ratio (SNR). The longer CPI of the orthogonal waveform mode accounts for the difference in probability of detection. It is seen that for SNR up to 8.5 dB, probability

of detection is almost identical. For SNR between 8.5 dB and 15 dB, the detection curves diverge. For SNR above 15 dB, probability of detection is equal to one for both modes. If a probability of detection of 0.9 is desired, the radar will require an additional 2 dB in SNR if orthogonal waveform mode is used.

Figure 3 compares probability of detection for a 16-element array. The separation between the detection curves is greater than for the 8-element case. In this case, the curves separate at 7 dB and do not converge until 14.5 dB. If a probability of detection of 0.5 is desired, then the radar will require an additional 0.5 dB if the use of orthogonal waveform mode is used. If a probability of detection of 0.9 is desired, the orthogonal waveform mode will require an additional 3.5 dB in SNR.

For a 24-element array, the probability of detection is compared in Figure 4. The separation between the detection curves is still more pronounced in this case, as the curves are separated for all values of SNR shown. An additional 1 dB is required for orthogonal waveform mode if the desired probability of detection is 0.5. However, for a probability of detection of 0.9, the orthogonal waveform mode will require an additional 4.5 dB in SNR.

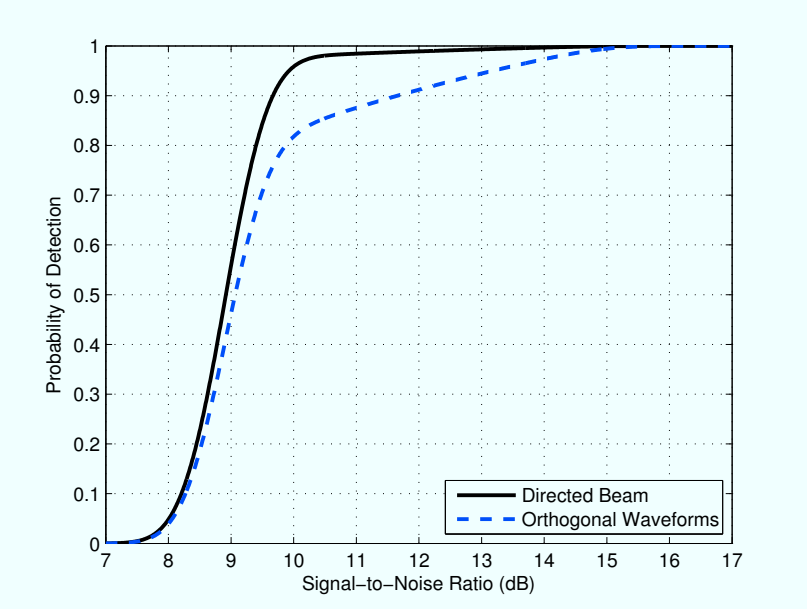

Figure 2: *Probability of detection for an 8-element array for* $P_{\text{fa}} = 10^{-5}$, $\rho = 30m$, *directed beam CPI length of 3.2 ms, and a target radial velocity of 250 m/s.*

4.2.2 Scenario 2

In Scenario 2, $\alpha_{\text{dir}}/\rho = 0.053$. The PRF is 10 kHz and the target radial velocity v is 500 m/s. For a directed beam, each CPI has 32 pulses, so that the CPI length is 3.2 ms. For

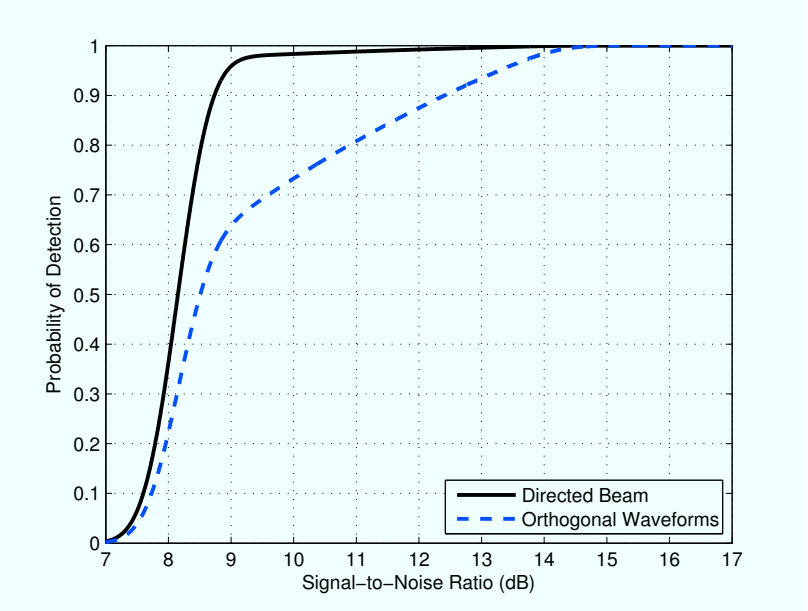

Figure 3: *Probability of detection for a 16-element array for* $P_{\text{fa}} = 10^{-5}$, $\rho = 30m$, *directed beam CPI length of 3.2 ms, and a target radial velocity of 250 m/s.*

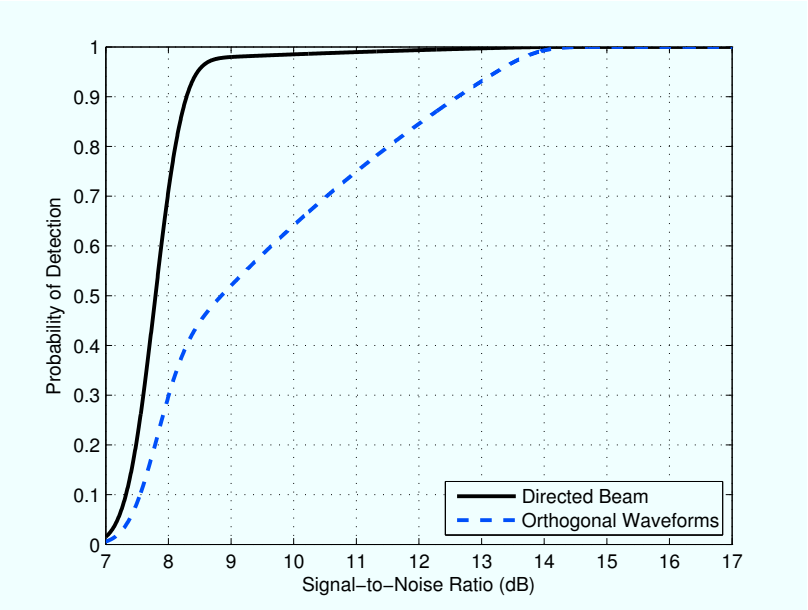

Figure 4: *Probability of detection for a 24-element array for* $P_{\text{fa}} = 10^{-5}$, $\rho = 30m$, *directed beam CPI length of 3.2 ms, and a target radial velocity of 250 m/s.*

antennas with 8, 16 and 24 elements, probability of detection for a directed beam will be compared to probability of detection for orthogonal waveforms. Table 2 shows the values of α and ρ. Scenario 2 is identical to Scenario 1, except that the target radial velocity has been doubled to 500 m/s.

Table 2: *Scenario 2: Distance travelled by the target during the CPI (α) and range cell length (ρ), in meters.*

Directed Beam	$\alpha_{\text{dir}} = 1.6$
Orthogonal Waveform (M=8)	$\alpha_{\text{orth}} = 12.8$
Orthogonal Waveform (M=16)	$\alpha_{\text{orth}} = 25.6$
Orthogonal Waveform (M=24)	$\alpha_{\text{orth}} = 38.4$
Range cell length	$\rho = 30$

In this scenario, the distance travelled by the target is less than the range cell length for directed beam mode and for orthogonal waveform mode when $M = 8$ and $M = 16$. However, for orthogonal waveform mode with $M = 24$, $\rho < \alpha_{\text{orth}} \leq 2\rho$. Thus for $M = 24$ the second line from (38) will be used to compute probability of detection.

Under Scenario 2 for an 8-element array, Figure 5 compares probability of detection for directed beam and orthogonal waveform modes. The two curves begin to separate significantly when directed beam SNR is greater than 9 dB. The curves converge again when SNR is 15 dB. If a probability of detection of 0.5 is desired, then orthogonal waveform mode will require an additional 0.3 dB in SNR. However, if the desired probability of detection is 0.9, then the additional SNR required for orthogonal waveform mode is 3.5 dB.

For a 16-element array, the probability of detection curves are shown in Figure 6. In this case, the curves are separated for values of SNR between 7 dB and 14.5 dB. For a desired probability of detection of 0.5, the additional SNR required for orthogonal waveforms is 2 dB, while for a desired probability of detection of 0.9, orthogonal waveform mode requires an additional 4.5 dB.

Figure 7 compares probability of detection for a 24-element array. There is significant separation between the curves, except for SNR less than 7 dB when probability of detection is zero and for SNR greater than 14 dB when probability of detection is one. If probability of detection of 0.5 is desired, orthogonal waveform mode requires an additional 3 dB in SNR. For a desired probability of detection of 0.9, an additional SNR of 5 dB in SNR is required if orthogonal waveforms are to be used. As noted earlier, $\rho < \alpha_{\text{orth}} \leq 2\rho$ for $M = 24$ whereas $\alpha_{\text{dir}} \leq \rho$. This is an indication of the difference in probability of detection is when the distance travelled by the target falls into different cases for (38).

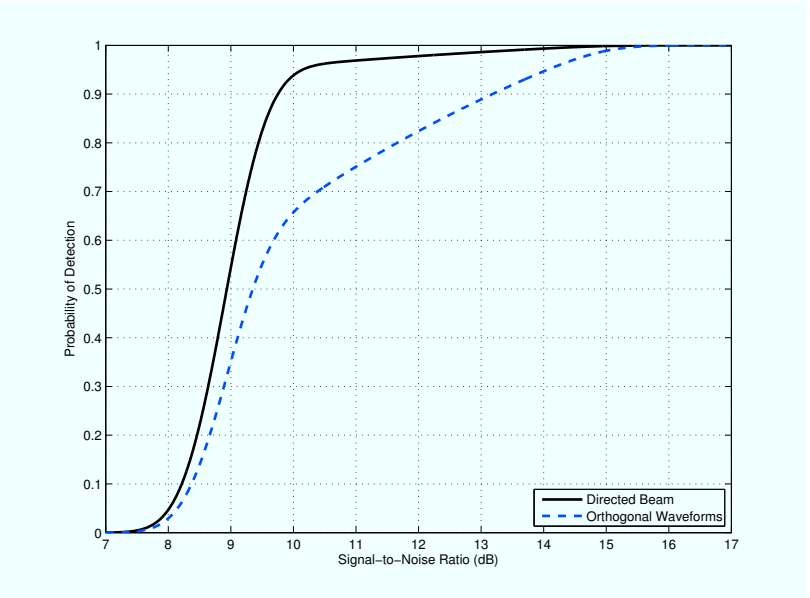

Figure 5: *Probability of detection for an 8-element array for* $P_{\text{fa}} = 10^{-5}$, $\rho = 30m$, *directed beam CPI length of 3.2 ms, and a target radial velocity of 500 m/s.*

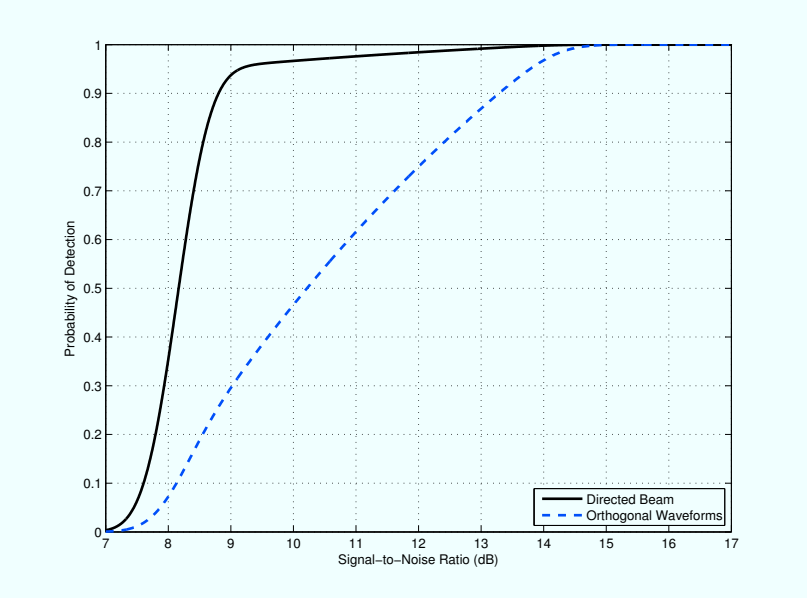

Figure 6: *Probability of detection for a 16-element array for* $P_{\text{fa}} = 10^{-5}$, $\rho = 30m$, *directed beam CPI length of 3.2 ms, and a target radial velocity of 500 m/s.*

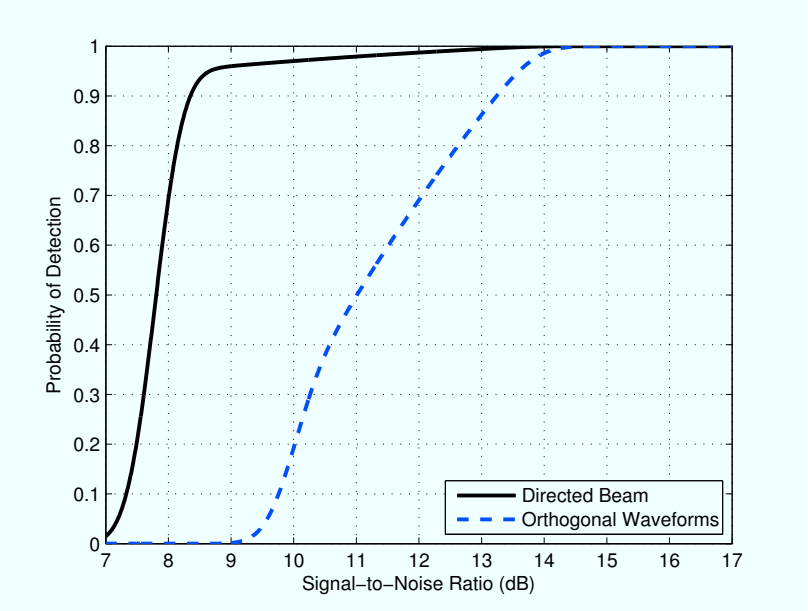

Figure 7: *Probability of detection for a 24-element array for* $P_{\text{fa}} = 10^{-5}$, $\rho = 30m$, *directed beam CPI length of 3.2 ms, and a target radial velocity of 500 m/s.*

4.2.3 Scenario 3

In Scenario 3, $\alpha_{\text{dir}}/\rho = 0.15$. The PRF is 5 kHz and the target radial velocity v is 700 m/s. For a directed beam, each CPI has 32 pulses, so that the CPI length is 6.4 ms. For antennas with 8, 16 and 24 elements, probability of detection for a directed beam will be compared to probability of detection for orthogonal waveforms. Table 3 shows the values of α and ρ. The pulse repetition interval is twice the PRI from Scenarios 1 and 2.

Table 3: *Scenario 3: Distance travelled by the target during the CPI* (α) *and range cell length* (ρ), *in meters.*

Directed Beam	$\alpha_{\text{dir}} = 4.48$
Orthogonal Waveform (M=8)	$\alpha_{\text{orth}} = 35.84$
Orthogonal Waveform (M=16)	$\alpha_{\text{orth}} = 71.68$
Orthogonal Waveform (M=24)	$\alpha_{\text{orth}} = 107.52$
Range cell length	$\rho = 30$

In this scenario, $\rho < \alpha_{\text{orth}} \leq 2\rho$ for $M = 16$ and $M = 24$ so that the total return from the target is spread over two or three range cells, depending on the starting point of the target.

Figure 8 shows probability of detection for an 8-element array. It is seen that the detection

curves have significant separation from 7.5 dB SNR to 15 dB SNR. For a desired probability of detection of 0.5, the orthogonal waveform mode requires an additional 3 dB in SNR. If a probability of detection of 0.9 is desired, then the use of orthogonal waveforms requires an additional 4 dB in SNR.

In Figure 9, probability of detection is compared for a 16-element array. In this case, $\alpha_{\text{orth}} = 71.68$ while $\rho = 30$ so that the target return is always spread over three range cells. As a result, there is significant spread between the detection curves. If a probability of detection of 0.5 is desired, then orthogonal waveform mode requires an additional 7.5 dB. Whereas an additional 6 dB is needed to achieve a probability of detection of 0.9.

Finally, probability of detection for a 24-element array is shown in Figure 10. There is a large separation between the curves in this case. To achieve a probability of detection of 0.5, orthogonal waveform mode requires an additional 11 dB in SNR. If a probability of detection of 0.9 is desired, an additional SNR of 10 dB is needed if orthogonal waveforms are used.

Note that for the directed beam detection curves in Scenario 3, the knee of the curve occurs for a probability of detection of approximately 0.88. This compares with the directed beam detection curves in Scenarios 1 and 2, where the knee of the curve occurs at 0.95.

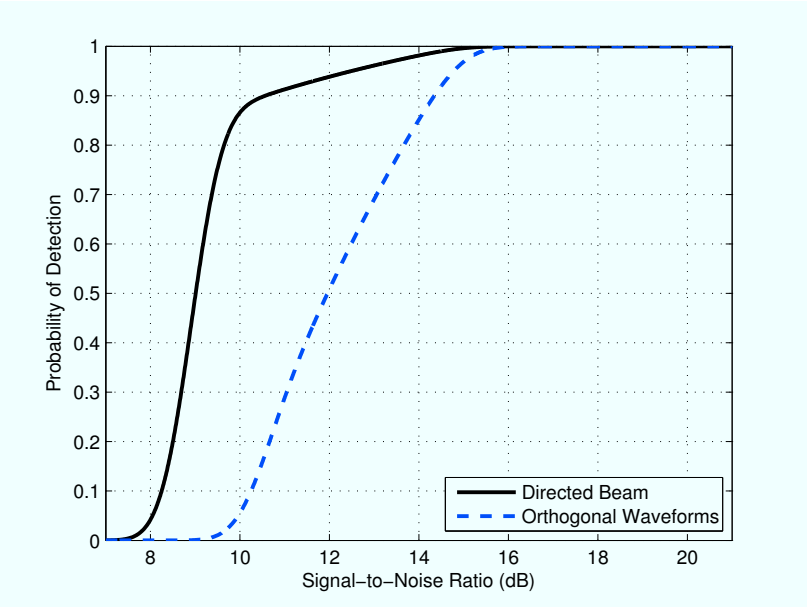

Figure 8: *Probability of detection for an 8-element array for $P_{\text{fa}} = 10^{-5}$, $\rho = 30m$, directed beam CPI length of 6.4 ms, and a target radial velocity of 700 m/s.*

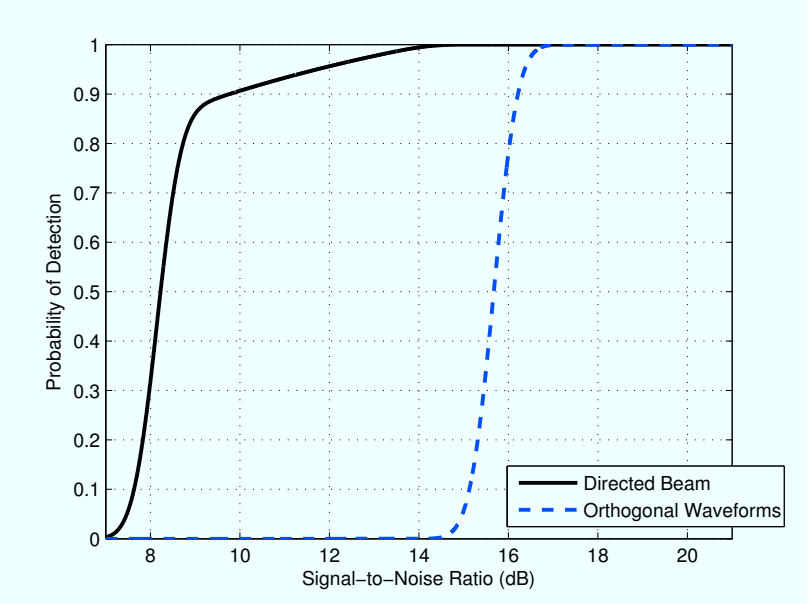

Figure 9: *Probability of detection for a 16-element array for* $P_{\text{fa}} = 10^{-5}$, $\rho = 30m$, *directed beam CPI length of 3.2 ms, and a target radial velocity of 500 m/s.*

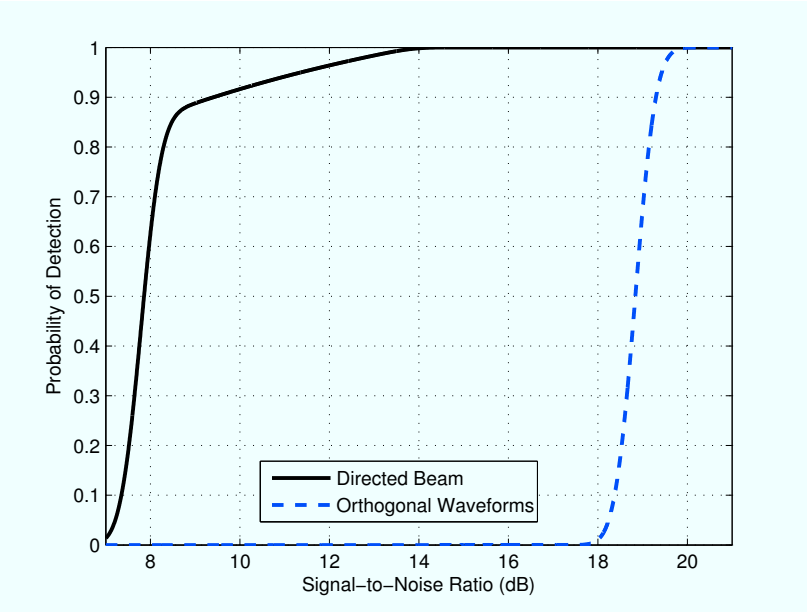

Figure 10: *Probability of detection for a 24-element array for* $P_{\text{fa}} = 10^{-5}$, $\rho = 30m$, *directed beam CPI length of 6.4 ms, and a target radial velocity of 700 m/s.*

4.3 Summary

The results from Scenarios 1, 2 and 3 indicate that the separation between probability of detection for directed beam and orthogonal waveform modes is monotonically increasing with α. It is also seen that the separation is monotonically increasing with the number of array elements M. Although a larger number of array elements enables greater flexibility for a MIMO radar, increasing the number of array elements also degrades probability of detection for high-velocity targets.

5 Evaluation of Search Strategies

In Section 4, the probability of detection for a directed beam mode was compared to probability of detection for an orthogonal waveform mode. In making this comparison, it was assumed that a single target with arbitrary velocity was to be detected and that the target was located in the center of the mainbeam for directed beam mode. The reduction in probability of detection for the orthogonal waveform mode was due to the longer integration time required.

This section considers a sector search, where the radar must scan a specified area, or sector, and search for targets that may be located at any position within the sector. In this section, it is assumed that the radar is a linear array, so that scanning is carried out in one dimension only, which is the case for horizon search for a naval radar.

In a directed beam search, the radar is electronically scanned so that subsequent radar beams cover a specified sector. The beams are positioned so that consecutive beams are separated by their 3-dB beamwidth. When the radar finishes scanning the sector it resumes at the beginning of the sector. It is assumed that the radar scans to ± 60 deg. The radar begins by directing a beam to -60 deg, scans across to $+60$ deg, and then returns to -60 deg to resume search of the sector again.

In MIMO search, the radar transmits orthogonal waveforms on each of the M array elements. The transmission is omnidirectional so that no steering is required. In order to maintain the same signal-to-noise ratio as the directed beam search, MIMO search uses an CPI length that is M times longer than that of the directed beam search. In MIMO radar search it is assumed that ideal orthogonal waveforms are generated and that signal processing is carried out at the receiver so that the received baseband signals are uncorrelated.

When comparing directed beam mode and orthogonal waveform mode for sector search, there are a number of factors that should be considered to make a fair comparison. Directed beam search suffers from three types of loss, which are as follows.

1. Beam shape loss,
2. Beam steering loss,
3. Sector search time lag.

Beam shape loss occurs because a target will not necessarily be located in the center of radar mainbeam. For sector search using directed beam mode, consecutive beams are separated by their 3-dB beamwidth. When a target is detected using directed beam mode, it may be located in the center of the mainbeam, 3-dB down in the beam or at any location in between. The target may be located at any position within the beam with equal probability. Compared to the ideal case of being located in the center of the mainbeam, a directed

beam is assumed to suffer a beam shape loss of 1.5 dB, on average. Since the orthogonal waveform mode does not use a directed beam, it does not suffer from beam shape loss.

Beam steering loss is the loss in antenna gain when the antenna is electronically steered away from boresite. When the antenna is steered to angle θ, the antenna gain is reduced by $\cos(\theta)$.

Sector search time lag occurs because a directed beam must sequentially cover the search sector via electronic steering. Although a given target may be in the detection range of the radar, there will be a time lag until the target is detected, because the directed beam radar must sequentially cover all beam positions in the sector. This sector search time lag decreases the effective detection range of the radar when a directed beam is used.

5.1 Effect of Beam Shape Loss Only

To illustrate a comparison between the two modes for sector search which accounts for beam shape loss only, consider an antenna array with 20 elements. In this example, $P_{\mathrm{d}} = 0.9$, $P_{\mathrm{fa}} = 10^{-5}$, and range cell length is 30 m. Three different directed beam CPI lengths are considered: 3 ms, 2 ms, and 1 ms. The corresponding orthogonal waveform CPI lengths are 60 ms, 40 ms, and 20 ms, respectively. For each CPI length and a specified target radial velocity, the signal-to-noise ratio required to achieve $P_{\mathrm{d}} = 0.9$ is computed for directed beam mode and orthogonal waveform mode, using (38). The SNR gain for directed beam mode is defined by

$$\text{SNR gain (directed beam)} = \frac{\text{SNR (directed beam)}}{\text{SNR (orthogonal waveform)}}$$

For directed beam mode, the SNR is determined by computing the SNR for the ideal case, when the target is located in the center of the mainbeam, and subtracting a beam shape loss of 1.5 dB. If SNR gain is greater than one, then directed beam mode has greater SNR. If SNR gain is less than one, then orthogonal waveform mode has greater SNR. Figure 11 shows how SNR gain varies with velocity for the CPI lengths considered. For all three values of CPI length, the SNR gain for the directed beam is less than 0 dB for lower velocities and greater than 0 dB for higher velocities. It is seen that the velocity for which SNR gain is 0 dB varies with CPI length. For longer CPI lengths, the plots cross 0 dB at a smaller value of velocity. For a CPI length of 3 ms, directed beam mode has larger SNR for targets with velocity greater than 80 m/s. However for a CPI length of 1 ms, a target must have a velocity of 250 m/s or greater for directed beam mode to have larger SNR.

5.2 Comparison for a Search Scenario

The sector search performance of the directed beam and orthogonal waveform modes is now compared for a scenario that is specified as follows. In this comparison, beam shape

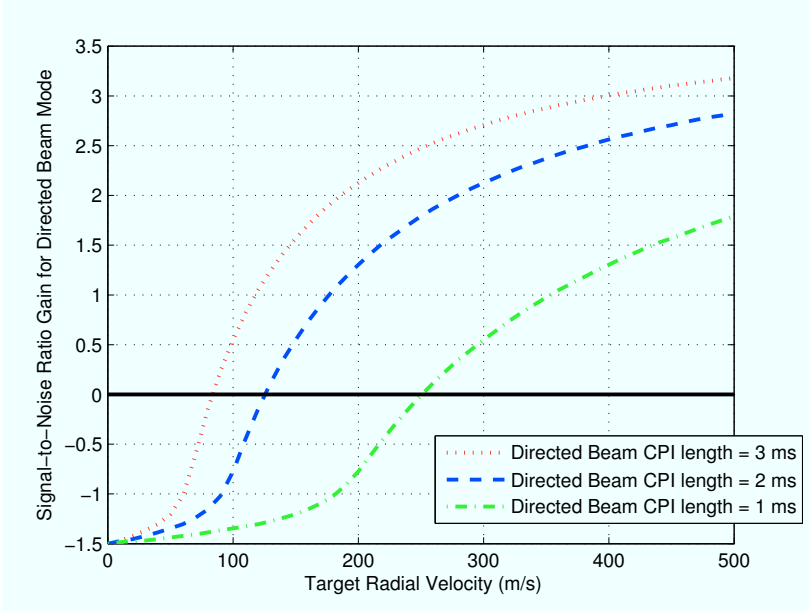

Figure 11: *SNR gain for directed beam mode for* $M = 20$, $P_{\mathrm{d}} = 0.9$, $P_{\mathrm{fa}} = 10^{-5}$, *and* $\rho = 30m$.

loss, beam steering loss, and sector search time lag are all taken into consideration. The radar is a 20-element horizontal linear array with a total horizontal dimension of 2 m and a vertical dimension of 0.25 m. In directed beam mode, the antenna electronically steers in azimuth to ± 60deg, which requires 138 beam positions, or dwells, to cover the sector. When a directed beam is used, 32 pulses per CPI are transmitted, with 3 CPIs per dwell. When orthogonal waveforms are used, 640 pulses are transmitted for each CPI. The desired probability of false alarm is 10^{-5} and the desired probability of detection is 0.9. Two different waveforms which transmit the same energy per pulse will be used, as specified in Table 4. Waveform 1 is a 20 μs pulse with 10 kW peak power and a 200 μs PRI, while Waveform 2 is a 10 μs pulse with 20 kW peak power and a 100 μs PRI.

Table 4: *Waveforms for search scenario.*

	Waveform 1	Waveform 2
Power (kW)	10	20
PRI (μs)	200	100
Pulse width (μs)	20	10

A number of targets are listed in Table 5. Each target is specified by its velocity, radar cross section (RCS) and angle of arrival relative to boresite of the antenna. For each target, the signal-to-noise ratio required to achieve the desired P_{d} and P_{fa} are computed using (38)

and (29), respectively. The corresponding detection range is then computed using the radar range equation, while accounting for beam shape loss, beam steering loss and sector search time lag when the directed beam mode is used. The target characteristics were chosen by design to be similar, so that the effects of varying velocity, RCS and angle of arrival can be easily seen.

A number of observations can be made from examining the detection range results from Table 5. Detection range for orthogonal waveform mode depends on target velocity and RCS but not on angle of arrival. Since, for example, targets 1 and 2 only differ in their angle of arrival, the orthogonal waveform detection range is identical for the two targets. Angle of arrival has an effect on directed beam detection range. The more the angle of arrival deviates from zero, the greater the beam steering loss, which decreases the detection range.

Targets 1 to 6 have zero radial velocity. Recall that Waveforms 1 and 2 transmit the same energy per pulse. For targets with zero radial velocity it is seen that there is no difference in detection range between Waveforms 1 and 2. The orthogonal waveform mode has greater detection range than directed beam mode. For targets 1, 3, and 5, which all have an angle of arrival of 0˚, directed beam is subject to beam shape loss in comparison to orthogonal waveforms. For targets 2, 4, and 6, which all have a non-zero angle of arrival, directed beam mode is also subject to beam steering loss.

Targets 7 to 12 have a radial velocity of 50 m/s. The choice of Waveforms 1 and 2 has negligible effect on detection range for directed beams; the difference is 0.1 km or less. Waveform choice has a significant effect on detection range for orthogonal waveforms, because Waveform 2 has a shorter CPI, which results in less range bin smearing. For targets 7, 9 and 11, which all have an angle of arrival of 0˚, orthogonal waveforms have a greater detection range than directed beams if Waveform 2 is used, but a smaller detection range than directed beams if Waveform 1 is used. For targets 8 and 10, which have angles of arrival of 45˚and -60˚, respectively, orthogonal waveform detection range is greater than directed beam detection range for both Waveforms 1 and 2. This is due to the beam steering loss suffered by the directed beam mode. For orthogonal waveforms the use of Waveform 2 increases detection range by approximately 10% compared to the use of Waveform 1.

For targets 13 to 18, which have a radial velocity of 100 m/s, the detection range of orthogonal waveforms relative to directed beam continues to degrade. The degradation is due to the higher velocity of the targets which cause the target return to be spread over multiple range cells. Targets 1, 7, and 13 have the same RCS and angle of arrival and differ only in velocity. It is seen that directed beam detection range varies negligibly with velocity and choice of Waveform 1 or 2. However, orthogonal waveform detection range decreases significantly as velocity increases. If Waveform 1 is used for targets 13 to 18, directed beam detection range is greater than orthogonal waveform detection range. If Waveform 2 is used, directed beam has greater detection range for targets 13, 15, 17, and 18, but orthogonal waveforms has greater detection range for targets 14 and 16, when the angle of

Table 5: *Target characteristics and detection ranges for search scenario.*

Target Number	Radial Velocity (m/s)	RCS (m^2)	Angle of Arrival (°)	Waveform 1 Detection Range (km)		Waveform 2 Detection Range (km)	
				Directed Beam	Orthogonal Waveform	Directed Beam	Orthogonal Waveform
1	0	5	0	115.7	126.2	115.7	126.2
2	0	5	45	106.1	126.2	106.1	126.2
3	0	1	0	77.4	84.4	77.4	84.4
4	0	1	-60	65.1	84.4	65.1	84.4
5	0	0.1	0	43.5	47.5	43.5	47.5
6	0	0.1	30	42.0	47.5	42.0	47.5
7	50	5	0	115.5	110.8	115.6	123.6
8	50	5	45	105.9	110.8	106.0	123.6
9	50	1	0	77.2	74.1	77.3	82.7
10	50	1	-60	64.9	74.1	65.0	82.7
11	50	0.1	0	43.4	41.7	43.5	46.5
12	50	0.1	30	41.9	41.7	41.9	46.5
13	100	5	0	115.3	101.5	115.5	110.8
14	100	5	45	105.8	101.5	105.9	110.8
15	100	1	0	77.1	67.9	77.2	74.1
16	100	1	-60	64.8	67.9	64.9	74.1
17	100	0.1	0	43.3	38.2	43.4	41.7
18	100	0.1	30	41.8	38.2	41.9	41.7
19	150	5	0	115.1	98.2	115.4	104.7
20	150	5	45	105.6	98.2	105.8	104.7
21	150	1	0	76.9	65.7	77.2	70.0
22	150	1	-60	64.7	65.7	64.9	70.0
23	150	0.1	0	43.2	36.9	43.3	39.4
24	150	0.1	30	41.6	36.9	41.8	39.4
25	250	5	0	114.6	96.6	115.2	99.6
26	250	5	45	105.1	96.6	105.7	99.6
27	250	1	0	76.5	64.6	77.0	66.6
28	250	1	-60	64.3	64.6	64.7	66.6
29	250	0.1	0	42.9	36.3	43.2	37.4
30	250	0.1	30	41.4	36.3	41.7	37.4
31	500	5	0	112.7	86.5	114.6	96.6
32	500	5	45	103.3	86.5	105.1	96.6
33	500	1	0	75.2	57.9	76.5	64.6
34	500	1	-60	63.1	57.9	64.3	64.6
35	500	0.1	0	42.0	32.5	42.9	36.3
36	500	0.1	30	40.5	32.5	41.4	36.3

arrival deviates the most from zero.

For targets 19 to 36, which have increasing target velocity, it is seen that much of same behaviour of detection range continues. Waveform 2 has larger detection range than Waveform 1. This difference is slight for directed beam but often significant for orthogonal waveforms. The difference in detection range between directed beams and orthogonal waveforms increases as velocity increases. This is consistent with observations from Section 4, where it was seen that the difference in SNR increased with velocity.

5.3 Summary

These results from the search scenario show that for lower-velocity targets, sector search using orthogonal waveforms has higher detection range. For high-velocity targets, sector search using a directed beam has higher detection range. The use of a shorter CPI duration reduces range bin smearing and improves probability of detection for orthogonal waveform mode.

6 Conclusions

The probability of detection for a radar using a directed beam was compared to the probability of detection for a radar using orthogonal waveforms. An analytical expression for the probability of detection in a single range cell was developed. For the detection of a single tracked target where the target location is known a priori, it is shown that the use of orthogonal waveforms results in lower probability of detection, because the longer integration time results in the target being spread over multiple range cells. As the number of antenna elements increases or target velocity increases, the difference in detection performance between directed beam and orthogonal waveforms increases.

For sector search, it is shown that the use of a directed beam results in a number of performance losses, including beam shape loss, beam steering loss, and sector search time lag. A search scenario is composed with targets that are specified by velocity, radar cross section, and angle of arrival. The use of orthogonal waveforms results in larger detection range for lower-velocity targets. For high-velocity targets, directed beam search has larger detection range. The choice of waveform has a significant impact on the detection performance of orthogonal waveforms. The use of a shorter coherent processing interval improves detection performance for orthogonal waveforms.

References

[1] Sévigny, Pascale (2008), Multiple-input multiple output MIMO radar: Literature survey of papers published between 2003 and September 2008, (DRDC Ottawa TM 2008-333) Defence R&D Canada – Ottawa.

[2] Rabideau, D.J. and Parker, P. (2003), Ubiquitous MIMO multifunction digital array radar, In *Conference Record of the Thirty-Seventh Asilomar Conference on Signals, Systems and Computers*, Vol. 1, pp. 1057–1064.

[3] Bekkerman, I. and Tabrikian, J. (2006), Target detection and localization using MIMO radars and sonars, *IEEE Trans. Signal Process.*, 54(10), 3873–3883.

[4] Rossum, W. L. Van and Huizing, A. G. (2007), Comparison of MIMO radar concepts: detection performance, In *Proc. of the IET International Conference on Radar Systems*, pp. 1–5.

[5] Li, Jian, Stoica, Petre, Xu, Luzhou, and Roberts, William (2007), On parameter identifiability of MIMO Radar, *IEEE Signal Process. Letters*, 14(12), 968–971.

DOCUMENT CONTROL DATA

(Security classification of title, body of abstract and indexing annotation must be entered when document is classified)

1. ORIGINATOR (The name and address of the organization preparing the document. Organizations for whom the document was prepared, e.g. Centre sponsoring a contractor's report, or tasking agency, are entered in section 8.)

   Defence R&D Canada – Ottawa
   3701 Carling Avenue, Ottawa, Ontario, Canada
   K1A 0Z4

2. SECURITY CLASSIFICATION (Overall security classification of the document including special warning terms if applicable.)

   UNCLASSIFIED

3. TITLE (The complete document title as indicated on the title page. Its classification should be indicated by the appropriate abbreviation (S, C or U) in parentheses after the title.)

   MIMO radar search strategies for high-velocity targets

4. AUTHORS (Last name, followed by initials – ranks, titles, etc. not to be used.)

   Moo, P.W.

5. DATE OF PUBLICATION (Month and year of publication of document.)	6a. NO. OF PAGES (Total containing information. Include Annexes, Appendices, etc.)	6b. NO. OF REFS (Total cited in document.)
March 2010	46	5

7. DESCRIPTIVE NOTES (The category of the document, e.g. technical report, technical note or memorandum. If appropriate, enter the type of report, e.g. interim, progress, summary, annual or final. Give the inclusive dates when a specific reporting period is covered.)

   Technical Memorandum

8. SPONSORING ACTIVITY (The name of the department project office or laboratory sponsoring the research and development – include address.)

   Defence R&D Canada – Ottawa
   3701 Carling Avenue, Ottawa, Ontario, Canada K1A 0Z4

9a. PROJECT NO. (The applicable research and development project number under which the document was written. Please specify whether project or grant.)	9b. GRANT OR CONTRACT NO. (If appropriate, the applicable number under which the document was written.)
11ag04	

10a. ORIGINATOR'S DOCUMENT NUMBER (The official document number by which the document is identified by the originating activity. This number must be unique to this document.)	10b. OTHER DOCUMENT NO(s). (Any other numbers which may be assigned this document either by the originator or by the sponsor.)
DRDC Ottawa TM 2009-288	

11. DOCUMENT AVAILABILITY (Any limitations on further dissemination of the document, other than those imposed by security classification.)

   (X) Unlimited distribution
   ( ) Defence departments and defence contractors; further distribution only as approved
   ( ) Defence departments and Canadian defence contractors; further distribution only as approved
   ( ) Government departments and agencies; further distribution only as approved
   ( ) Defence departments; further distribution only as approved
   ( ) Other (please specify):

12. DOCUMENT ANNOUNCEMENT (Any limitation to the bibliographic announcement of this document. This will normally correspond to the Document Availability (11). However, where further distribution (beyond the audience specified in (11)) is possible, a wider announcement audience may be selected.)

   Full unlimited announcement.

13. ABSTRACT (A brief and factual summary of the document. It may also appear elsewhere in the body of the document itself. It is highly desirable that the abstract of classified documents be unclassified. Each paragraph of the abstract shall begin with an indication of the security classification of the information in the paragraph (unless the document itself is unclassified) represented as (S), (C), (R), or (U). It is not necessary to include here abstracts in both official languages unless the text is bilingual.)

This work considers the detection of high-velocity targets for naval phased array radar. The detection performance of multiple-input multiple-output (MIMO) radar with orthogonal waveforms is compared to that of a radar using a directed beam. An analytical expression for the probability of detection for a radar with a multiple element array is derived. For high velocity targets, the decrease in probability of detection due to the longer integration time required for MIMO radar is quantified. It is shown that for lower-velocity targets, sector search using orthogonal waveforms results in higher detection range. For higher-velocity targets, the use of scanning directed beams yields higher detection range.

14. KEYWORDS, DESCRIPTORS or IDENTIFIERS (Technically meaningful terms or short phrases that characterize a document and could be helpful in cataloguing the document. They should be selected so that no security classification is required. Identifiers, such as equipment model designation, trade name, military project code name, geographic location may also be included. If possible keywords should be selected from a published thesaurus. e.g. Thesaurus of Engineering and Scientific Terms (TEST) and that thesaurus identified. If it is not possible to select indexing terms which are Unclassified, the classification of each should be indicated as with the title.)

Multiple-input multiple-output (MIMO) radar
Target detection
High-velocity targets

Defence R&D Canada

Canada's leader in Defence
and National Security
Science and Technology

R & D pour la défense Canada

Chef de file au Canada en matière
de science et de technologie pour
la défense et la sécurité nationale

www.drdc-rddc.gc.ca